ACS APPLIED MATERIALS & INTERFACES

Research Article

www.acsami.org

Triple Shape Memory Effects of Cross-Linked Polyethylene/Polypropylene Blends with Cocontinuous Architecture

Jun Zhao,[†] Min Chen,[†] Xiaoyan Wang,[†] Xiaodong Zhao,[†] Zhenwen Wang,[†] Zhi-Min Dang,*[,†] Lan Ma,*[,‡] Guo-Hua Hu,*[,§] and Fenghua Chen[∥]

[†]Department of Polymer Science and Engineering, School of Chemistry and Biological Engineering, University of Science and Technology Beijing, Beijing 100083, P. R. China

[‡]Department of Chemical Engineering, Texas Tech University, Lubbock, Texas 79409, United States

[§]CNRS-Universté de Lorraine, Laboratoire Réactions et Génie des Procédés, UMR 7274, ENSIC, 1 rue Grandville, BP 20451, Nancy, F-54000, France

[∥]Beijing National Laboratory for Molecular Sciences, Joint Laboratory of Polymer Science and Materials, CAS Key Laboratory of Engineering Plastics and State Key Laboratory of Polymer Physics and Chemistry, Institute of Chemistry, Chinese Academy of Sciences, Beijing 100190, P. R. China

ABSTRACT: In this paper, the triple shape memory effects (SMEs) observed in chemically cross-linked polyethylene (PE)/polypropylene (PP) blends with cocontinuous architecture are systematically investigated. The cocontinuous window of typical immiscible PE/PP blends is the volume fraction of PE (v^{PE}) of ca. 30−70 vol %. This architecture can be stabilized by chemical cross-linking. Different initiators, 2,5-dimethyl-2,5-di(*tert*-butylperoxy)-hexane (DHBP), dicumylperoxide (DCP) coupled with divinylbenzene (DVB) (DCP−DVB), and their mixture (DHBP/DCP−DVB), are used for the cross-linking. According to the differential scanning calorimetry (DSC) measurements and gel fraction calculations, DHBP produces the best cross-linking and DCP−DVB the worst, and the mixture, DHBP/DCP−DVB, is in between. The chemical cross-linking causes lower melting temperature (T_m) and smaller melting enthalpy (ΔH_m). The prepared triple shape memory polymers (SMPs) by cocontinuous immiscible PE/PP blends with v^{PE} of 50 vol % show pronounced triple SMEs in the dynamic mechanical thermal analysis (DMTA) and visual observation. This new strategy of chemically cross-linked immiscible blends with cocontinuous architecture can be used to design and prepare new SMPs with triple SMEs.

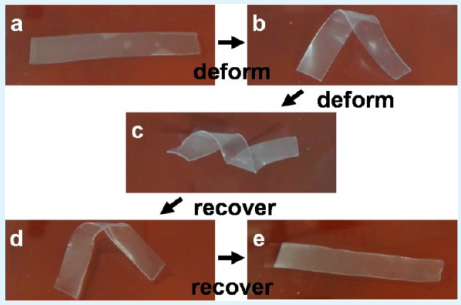

KEYWORDS: *shape memory polymer, polyolefin, multiple actuation, chemical cross-linking*

1. INTRODUCTION

Shape memory materials show the "memorizing" ability by recovering to their permanent shape under the external stimuli (such as temperature change, humidity change, and electromagnetic fields) from their temporary shape which is usually formed by deformation under load and can be kept for quite a long time after deformation and unloading.[1] Such an ability gives shape memory materials great potential to be used as sensors, actuators, and biomedical devices. However, the current widely used shape memory materials, mainly shape memory alloys (SMAs) and shape memory ceramics (SMCs), have some obvious disadvantages such as low strain (usually less than 8%), high response temperature, high density, and difficult processing.[1] Therefore, shape memory polymers (SMPs) that can overcome the disadvantages of the SMAs and SMCs have emerged as a new candidate of shape memory materials.[2−8] Generally speaking, SMPs are composed of two different domains: the first one (fixed domain) that can be used to keep the permanent shape is often chemical or physical cross-linking points, and the second one (reversible domain) that can be used to form the temporary shape is often an amorphous or a crystalline phase.

For the shape memory effect (SME) of SMPs, the switch temperature (T_{sw}) of the reversible domain is crucial and can be glass transition temperature (T_g) for the amorphous phase or melting temperature (T_m) for the crystalline phase. At temperature above the T_{sw}, the molecular chains in the reversible domain have the mobility and can be deformed under force. As a result, the shape can be changed from curled to stretched. Then the deformation can be fixed or frozen by cooling to temperatures below the T_{sw} under the external tension. When the force is unloaded, the temporary shape is ideally fixed with no loss in strain. Finally, when the temperature is increased above the T_{sw} without external tension, the molecular chains can release the deformation and recover to their permanent shape due to their high enough mobility. Therefore, the primary driving force for the SME is

Received: February 28, 2013
Accepted: May 28, 2013
Published: May 28, 2013

   dx.doi.org/10.1021/am400769j | *ACS Appl. Mater. Interfaces* 2013, 5, 5550−5556

actually entropic in nature since the polymer chains energetically prefer to return to the most disordered conformation.

In the past decade, substantial efforts in the field of SMPs have been focused on the following several hot directions such as SMP composites with reinforcing or functional fillers to increase the mechanical and thermal properties or to realize long-distance triggering,[9−16] SMPs with biocompatibility and/or biodegradability to be used in the biological or medical field,[17,18] and two-way reversible SMPs that can remember both high and low temperature shapes and are very useful for the reversible actuation in artificial muscles and actuators.[19−25]

Compared with the traditional double SMPs that have only one permanent shape and one temporary shape, triple SMPs have one permanent shape and two temporary shapes.[10] Therefore, triple SMPs can provide more complex actuation than double SMPs. While double SMPs only need one reversible phase, triple SMPs generally need two reversible phases. On the basis of this principle, many different strategies have been proposed to prepare triple SMPs. The chemical methods include graft or block copolymerization[21,26−28] and chemical cross-linking coupled with supramolecular bonding.[29] The physical methods are mainly physical cross-linking of multiple crystalline polymers[30] and bilayer structure of two double SMPs with well-separated T_{sw}'s.[14,31] Side-chain liquid crystalline networks can also be used to prepare triple SMPs.[32] It is also interesting that multiple SMPs can be obtained from polymers with broad glass transition.[33−35]

In the past decades, mixing existing polymers with each other to get polymer blends has become a widely accepted practice to obtain new materials with desirable properties. The architecture of polymer blends is critical to the materials' properties. Actually, only a few polymer couples are completely or partially miscible; most are completely immiscible. For the immiscible binary polymer blends, the most important architectures are sea-island architecture and cocontinuous architecture. For the polymer blends with sea-island architecture, in which one component (island phase) is dispersed in the continuous matrix (sea phase) of another component, the properties of the continuous (sea) phase are usually dominant in the materials' properties. As a comparison, for the polymer blends with cocontinuous architecture, in which each component forms a three-dimensionally percolating network, both components can be taken as the continuous matrix, and the specifically good properties of both components could probably be synergically combined.[36−39] Actually, the cocontinuous architecture has played an important role in the design of some novel materials to enhance the mechanical, electronic, optical, and transporting properties (e.g., the light absorption and electricity production layers of polymer solar cells in which donor and acceptor domains must contact each other with a favorite distance of 10−20 nm[40,41] and the membranes of fuel cells where smooth pathways for masses' moving are needed[42−44]).

In this work, cocontinuous architecture is first built up in immiscible polyethylene (PE)/polypropylene (PP) blends, and then triple SMPs are prepared by chemical corss-linking of the blends. The employment of the cocontinuous architecture is for the synergetic enhancement of mechanical properties. Considering the fact that PE and PP are the most important general plastics with mass production and a substantial cost advantage, the prepared materials might have good potential applications.[13,45] This new strategy of chemically cross-linked immiscible blends with cocontinuous architecture might be helpful to the design and preparation of new SMPs with triple SMEs.

2. EXPERIMENTAL SECTION

2.1. Materials. Some of the materials used in this work were the same as those in our previous work.[16] PE (type LD100BW) and PP (type K7726) pellets purchased from Sinopec Beijing Yanshan Company (China) had the density of 0.923 g cm^{-3} and 0.901 g cm^{-3}, respectively, and the melt flow index of 2.0 g (10 min)$^{-1}$ and 10 g (10 min)$^{-1}$, respectively. 2,5-Dimethyl-2,5-di(*tert*-butylperoxy)-hexane (DHBP, 92% purity), dicumylperoxide (DCP, 98% purity), and divinylbenzene (DVB, >50% purity) were obtained from Acros Organics (Belgium), Sigma-Aldrich (USA), and Tokyo Chemical Industry (Japan), respectively. Xylene (AR) was purchased from Beijing Chemical Plant (China).

2.2. Sample Preparation. Procedures similar to our previous work were used.[16] PE pellets and PP pellets were completely dried in a vacuum oven at 80.0 °C overnight before they were mixed in a Thermal Scientific Haake MiniLab II mixer (Germany) at 170.0 °C and 60 rpm for 10 min. The mixtures were then extruded and cut into pieces before they were soaked by ca. 5 wt % (relative to the total polymer mass) initiators of DHBP, DCP−DVB (weight ratio of 1/1, DCP dissolved by DVB), or the mixture of DHBP/DCP−DVB (weight ratio of 1/2) in a hermetic glass flask at room temperature of 25.0 °C for 72 h. The soaked sample pieces were subsequently molded by hot pressing at 170.0 °C and 20.0 MPa for 30 min to get both PE and PP components cross-linked. Finally, slow cooling in air of the samples was used to get the thin films with the thickness of 0.5−1.0 mm.

2.3. Gel Weight Fraction (f_g^w) Measurements. The procedure used here was similar to our previous work.[16] The f_g^w represents the weight fraction of cross-linked polymer components in the samples. Samples of 0.05−0.1 g were immersed in a relatively large volume of xylene and gently stirred at 95.0 °C to selectively extract the un-cross-linked linear polymer component until the samples reached a constant weight. Then the extracted samples were dried completely in a vacuum oven at 80 °C overnight, and the weight was checked. The equation of the quantitative data on the f_g^w was as follows

$$f_g^w = \frac{w_f}{w_i} \times 100\% \quad (1)$$

where w_i and w_f were the weight of the sample before and after the solvent extraction. For the reproducibility, all the reported values were the average of at least three different samples with the same composition and the same processing conditions.

2.4. Scanning Electron Microscopy (SEM) Observation. The procedure used here was similar to our previous work.[16] The un-cross-linked PE/PP blends with various compositions were fractured in liquid nitrogen and then immersed in a relatively large volume of xylene at 90.0 °C for 10 min before they were taken out and completely dried in a vacuum oven at 80.0 °C overnight. Then the surface was sputtered with thin gold film. Architecture observation was carried out on a Hitachi S4700 SEM (Japan) running at an accelerating voltage of 20 kV.

2.5. Differential Scanning Calorimetry (DSC) Measurements. The procedure used here was similar to our previous work.[16] DSC measurements were performed on a Shimadzu DSC-60 (Japan) under nitrogen atmosphere. Both the temperature and enthalpy were calibrated with indium. The samples of 5−10 mg were dried in a vacuum oven at 80 °C before they were sealed in aluminum crucibles. The samples were heated from room temperature of 25.0 to 200.0 °C at 10.0 K min^{-1}. The degree of crystallinity (X_c) for the samples was calculated as follows

$$X_c = \frac{\Delta H_m}{\Delta H_m^{\infty} w} \times 100\% \quad (2)$$

where ΔH_m and ΔH_m^{∞} were the melting enthalpy of one polymer component and that of its perfect polymer crystals (ca. 277.1 J g^{-1} for

dx.doi.org/10.1021/am400769j | ACS Appl. Mater. Interfaces 2013, 5, 5550−5556

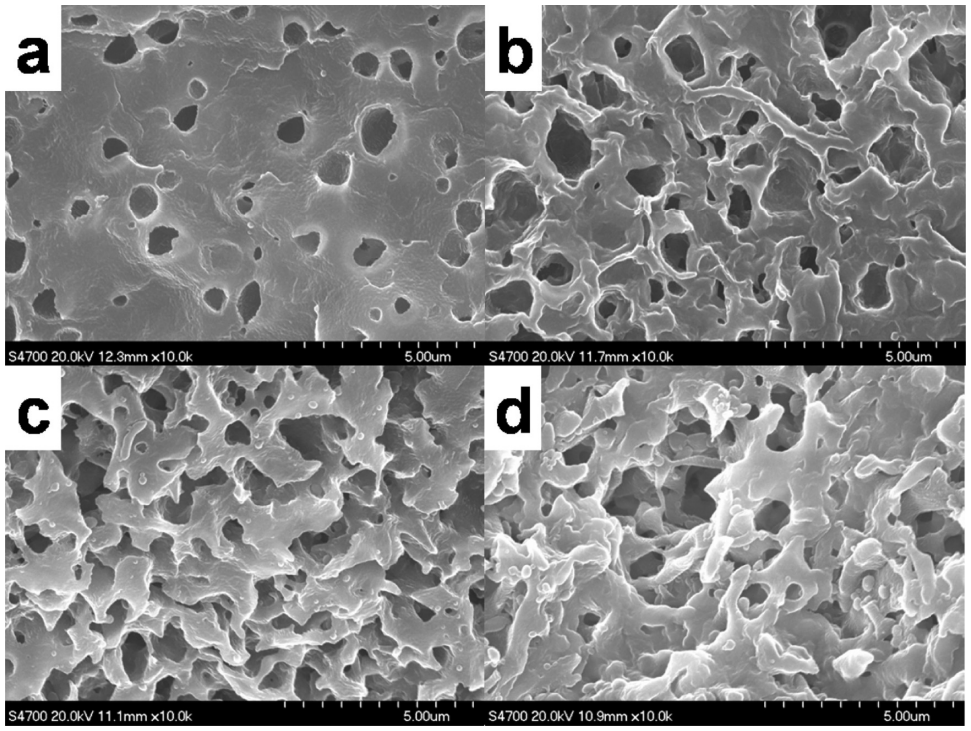

Figure 1. SEM micrographs of the cryo-fractured surface of un-cross-linked PE/PP blends with various v^{PE}: 10 vol % (a), 30 vol % (b), 50 vol % (c), and 70 vol % (d). PE has been extracted with xylene.

PE and ca. 185.7 J g^{-1} for PP, respectively),[46] and w was the weight fraction of the polymer component in the blends.

2.6. Dynamic Mechanical Thermal Analysis (DMTA) Measurements and Shape Memory Effect (SME) Analysis. The measurements used here was similar to our previous work.[16] The traditional DMTA measurements were carried out by using a dynamic mechanical thermal analyzer (TA Instruments Q800, USA) in the tension mode with the temperature range from room temperature of 25.0 to 250.0 °C, heating rate of 3.0 K min^{-1}, and frequency of 1 Hz. The samples with thickness of 0.5−1.0 mm were cut into rectangular shape with width of ca. 3.0 mm and length of more than 20.0 mm. The initial clamp gap and strain were set to be ca. 5.0 mm and 0.05%. The low heating/cooling rate of 3.0 K min^{-1} was employed in these measurements to reduce the temperature gradient in the samples.

For the SME analysis of the prepared SMP samples, a four-step program on the dynamic mechanical thermal analyzer was employed. In the first step, the samples were first kept isothermal at 170.0 °C for 5 min before they were stretched with the stress increase from 0 to 0.0025 MPa in 2 min. Then the samples were cooled to 120.0 °C at 3.0 K min^{-1} under the stress of 0.0025 MPa. In the second step, the stress was unloaded in 2 min, and then the samples were kept isothermal for 10 min before the stress was increased to 0.25 MPa in 2 min. Afterward, the samples were cooled to 45.0 °C at 3.0 K min^{-1} under the stress of 0.25 MPa. In the third step, the stress was unloaded in 2 min, and then the samples were heated to 120.0 °C at 3.0 K min^{-1} without load. Afterward, the samples were kept isothermal for 10 min. In the fourth step, the samples were heated further to 170.0 °C at 3.0 K min^{-1} and then kept isothermal for 10 min. This cycle was repeated at least three times for the reproducibility of SME.

Strain fixity ratio (R_f) and strain recovery ratio (R_r) were two crucial parameters to describe the triple SMEs of the samples with two temporary shapes, x and y. The R_f for the temporary shape x ($R_f(x)$) and the R_r for the recovery from temporary shape y to x ($R_r(y\rightarrow x)$) were calculated as follows[10,45]

$$R_f(x) = \frac{\varepsilon_x}{\varepsilon_{x,load}} \times 100\% \quad (3)$$

$$R_r(y \rightarrow x) = \frac{\varepsilon_y - \varepsilon_{y,rec}}{\varepsilon_y - \varepsilon_x} \times 100\% \quad (4)$$

where ε_x, ε_y, $\varepsilon_{x,load}$, and $\varepsilon_{y,rec}$ were the strain (ε) after unloading for shape x, after unloading for shape y, before unloading for shape x, and after recovery for shape y, respectively. The R_f for the temporary shape y ($R_f(y)$) and the R_r for the recovery from temporary shape x to the permanent shape ($R_r(x\rightarrow 0)$) were calculated in a similar way.

3. RESULTS AND DISCUSSION

Figure 1 shows SEM micrographs of the cryo-fractured surface of PE/PP blends with various v^{PE}. It should be mentioned that although xylene is a good solvent for both PE and PP at high enough temperature, e.g., 95.0 °C (long time is also needed), PE is more soluble than PP at lower temperature of 90.0 °C due to the much lower T_m of PE (ca. 109 °C) than that of PP (ca. 165 °C). Therefore, PE can be selectively dissolved after a short time of 10 min, while most of the PP remains undissolved. It can be seen from Figure 1 that for the blends with v^{PE} of 10 vol % the PE component is the dispersed phase with diameter of several micrometers, while the PP component is the continuous matrix, which is a typical sea-island architecture. For the blends with v^{PE} of 30 vol %, the PP component is still the continuous matrix. Although some dispersed phase of PE can be seen, most of the PE already forms a continuous phase. For the blends with v^{PE} of 50 vol %, both PE and PP components are the continuous matrix. Therefore, well-defined cocontinuous architecture is formed in the system for this composition. For the blends with v^{PE} of 70 vol %, the PE component is the continuous matrix. For this composition, although most of the PP is still continuous phase, some dispersed phase of PP can already be seen. For the blends with v^{PE} of 90 vol %, the PE component is the continuous matrix, while the PP component is the dispersed phase with diameter of several micrometers (SEM micrographs not given).

According to these results, it is clear that the cocontinuous window of PE/PP blends is the v^{PE} of ca. 30−70 vol %, and the best cocontinuous architecture is formed for the v^{PE} of ca. 50 vol %. It is plausible to assume that the cocontinuous architecture will be preserved after chemical cross-linking of the blends.

Scheme 1 presents the chemical structures of DHBP, DCP, and DVB, where DHBP and DCP are two kinds of initiators

Scheme 1. Schematic Presentation of the Chemical Structures of DHBP, DCP, and DVB

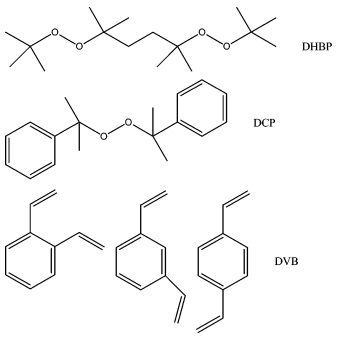

with peroxy groups while DVB is an assistant cross-linking agent for DCP initiation. Both of these initiators have been used for the cross-linking of polyolefins including PE and PP.[13,45] According to our previous work, DHBP is an efficient cross-linking agent for PE samples because it is fluid at room temperature and can be absorbed by PE, and its reaction efficiency is high at high temperature of 170−200 °C.[16] The cross-linking reaction occurring by the decomposition of both DHBP and DCP is to produce reactive oxygen radicals, which can react with and connect PE and/or PP chains. As will be given later in detail, for the PE/PP blends, DHBP produces the highest f_g^w and DCP−DVB the lowest, and DHBP/DCP-DVB is in between. The reason might be due to not only the absorption of initiators by the polymer matrix but also to the decomposition efficiency of the initiators.

Figure 2a shows the DSC heat flow (HF) traces of linear and cross-linked PE, PP, and PE/PP blends with v^{PE} of 50 vol % initiated by DHBP during heating. It can be seen that both linear PE (*l*PE) and linear PP (*l*PP) have a single melting peak at ca. 108.5 °C and ca. 164.9 °C, respectively. The degree of crystallinity (X_c) measured by DSC for pure *l*PE and pure *l*PP is ca. 28.7% and ca. 45.1%, respectively. For the linear PE/PP (*l*PE/*l*PP) blends, the two melting peaks are at ca. 108.1 °C and ca. 165.1 °C, respectively, which are very close to that of the pure components. Besides, the X_c of two components is 23.7% and 35.3%, respectively, which are also very close to that of the pure components. These results clearly indicate the almost complete immiscibility between PE and PP components in the blends. After chemical cross-linking, the melting peak of PE shifts down to ca. 98.9 °C while that of PP to ca. 161.1 °C. The X_c of cross-linked PE (*c*PE) and cross-linked PP (*c*PP) is 20.3% and 38.7%, respectively. For the cross-linked PE/PP (*c*PE/*c*PP) blends, the melting peaks are at ca. 94.1 °C and ca. 154.5 °C, respectively. The X_c of two cross-linked components is 18.3% and 23.6%, respectively. These results clearly indicate that the chemical cross-linking hinders the crystallization of both components.

Figure 2b presents the temperature dependence of storage Young's modulus (E') in *c*PE, *c*PP, and *c*PE/*c*PP blends with v^{PE} of 50 vol % during heating. For both *c*PE and *c*PP, there is only a single step at ca. 113 °C and ca. 174 °C, respectively. For the *c*PE/*c*PP blends, there are double steps at ca. 111 °C and ca. 172 °C, respectively, which also indicates the almost complete immiscibility between PE and PP. Actually, the stepwise decrease of E' is the characteristic of cross-linked systems.[16] Therefore, the double E' steps in Figure 2b clearly indicate that both PE and PP components in the blends are chemically cross-linked. Such samples can be used as triple SMPs with two T_{sw}'s of ca. 110 °C and ca. 170 °C.

Figure 3a presents DSC HF traces of linear and cross-linked PE/PP blends with v^{PE} of 50 vol % initiated by different initiators during heating. It can be seen that all the initiators cause the decrease of both T_m and X_c. Among three initiators, DHBP has the most significant effect and DCP−DVB the least effect, and the initiator mixture of DHBP/DCP−DVB is in between.

Figure 3b presents the temperature dependence of E' in cross-linked PE/PP blends with v^{PE} of 50 vol % initiated by different initiators during heating. Double E' steps can be seen for all three initiators. It also clearly indicates that DHBP produces the most pronounced double E' steps and DCP−DVB the least pronounced steps, and DHBP/DCP−DVB is in between. The f_g^w's of these three samples are measured to be 95.5%, 84.3%, and 94.3%, respectively, which is in agreement with the DSC and DMTA measurements.

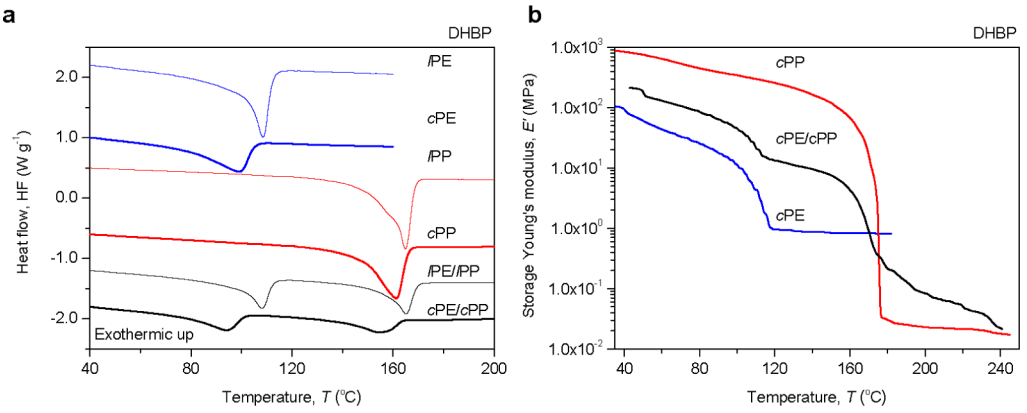

Figure 2. DSC thermographs showing HF of linear and cross-linked PE, PP, and PE/PP blends with v^{PE} of 50 vol % initiated by DHBP during heating (a) and temperature dependence of E' in cross-linked PE, PP, and PE/PP blends with v^{PE} of 50 vol % during heating (b).

dx.doi.org/10.1021/am400769j | ACS Appl. Mater. Interfaces 2013, 5, 5550−5556

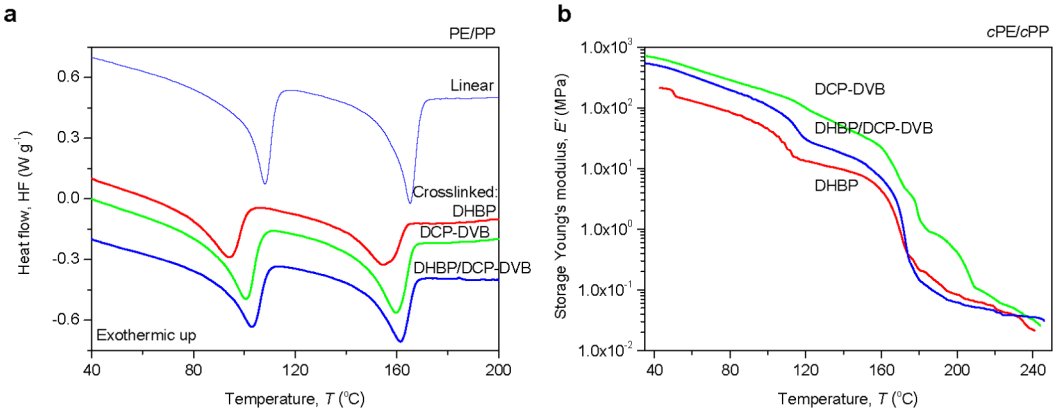

Figure 3. DSC thermographs showing HF of linear and cross-linked PE/PP blends with v^{PE} of 50 vol % initiated by different initiators during heating (a) and temperature dependence of E' in cross-linked PE/PP blends with v^{PE} of 50 vol % initiated by different initiators during heating (b).

Figure 4 presents the time dependence of temperature (T), stress (σ), and strain (ε) during the triple SME cycle of cross-linked PE/PP blends with v^{PE} of 50 vol % initiated by DHBP. The process is divided into four steps. In the first step, when σ of 0.0025 MPa is loaded at 170.0 °C, the ε is increased to ca. 6.1% quickly. During the cooling at 3.0 K min^{-1} to 120.0 °C under the load, there is nearly no change of ε. In the second step, the σ is unloaded, and the ε decreases slightly to ca. 4.7%. Afterward, σ is increased to 0.25 MPa at 120.0 °C, and the ε is increased to ca. 12.8% quickly. During the cooling at 3.0 K min^{-1} to 45.0 °C under the load, there is a slight decrease of ε to ca. 11.0%. Then the σ is unloaded, and the ε decreases further to 9.5%. The two steps above are the deformation process, and the following two steps are the recovery process by heating without load. In the third and fourth steps, the ε first decreases to ca. 6.5% at 120.0 °C and then to ca. 2.8% at 170.0 °C. Considering the fact that the ε is still decreasing during the isothermal stay at 170.0 °C, the R_r could reach a higher value after longer isothermal stay. The $R_f(x)$, $R_f(y)$, $R_r(y\rightarrow x)$, and $R_r(x\rightarrow 0)$ for this cycle of triple SMEs are ca. 77%, ca. 86%, ca. 88%, and ca. 79%, respectively. The standard deviation for these quantities during three consecutive cycles was ca. 10%. This DMTA program clearly shows the triple SMEs of cross-linked PE/PP blends.

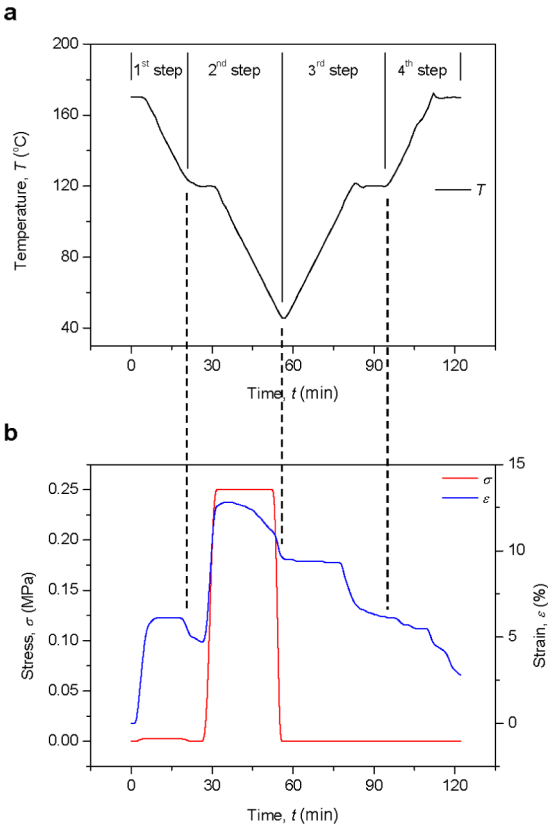

Figure 4. Time dependence of T (a) and σ and ε (b) during the triple SME cycle of cross-linked PE/PP blends with v^{PE} of 50 vol % initiated by DHBP. The four steps are also indicated.

Figure 5 presents the photographs of cross-linked PE/PP blends with v^{PE} of 50 vol % initiated by DHBP in the triple SME cycle of deformation and recovery. The two temporary shapes are formed at 175.0 and 130.0 °C in sequence. In the following recovery process by heating, the first temporary shape and permanent shape can be recovered in a reverse order, at 130.0 and 175.0 °C, respectively. It can be seen that the recovery of both the first temporary shape and the permanent shape is almost complete. Therefore, well-defined triple SMPs are prepared in this work.

Considering the fact that two components of blends are usually used as fixed phase and reversible phase, respectively, to prepare double SMPs,[13,47] our strategy of first blending two immiscible polymer components to form cocontinuous architecture and then chemically cross-linking both components provides a flexible approach to realize triple SMEs. A very recent literature on the chemically cross-linked semicrystalline polymer blends of PE/polycyclooctene (PCO) also demonstrated triple SMEs.[48] However, there was no purposeful control on the microarchitecture of the blends.[48] Actually, the cocontinuous architecture could synergically combine the specific properties of both components in a right way and provide the favorable mechanical properties of the blends.

4. CONCLUSIONS

The triple SMEs observed in chemically cross-linked PE/PP blends with cocontinuous architecture have been systematically investigated. The cocontinuous window of typical immiscible PE/PP blends was the v^{PE} of ca. 30−70 vol %. This architecture could be stabilized by the following chemical cross-linking. Different initiators, DHBP, DCP−DVB, and DHBP/DCP−DVB, were used for the cross-linking. According to the DSC measurements and f_g^w calculations, DHBP produced the best

dx.doi.org/10.1021/am400769j | ACS Appl. Mater. Interfaces 2013, 5, 5550−5556

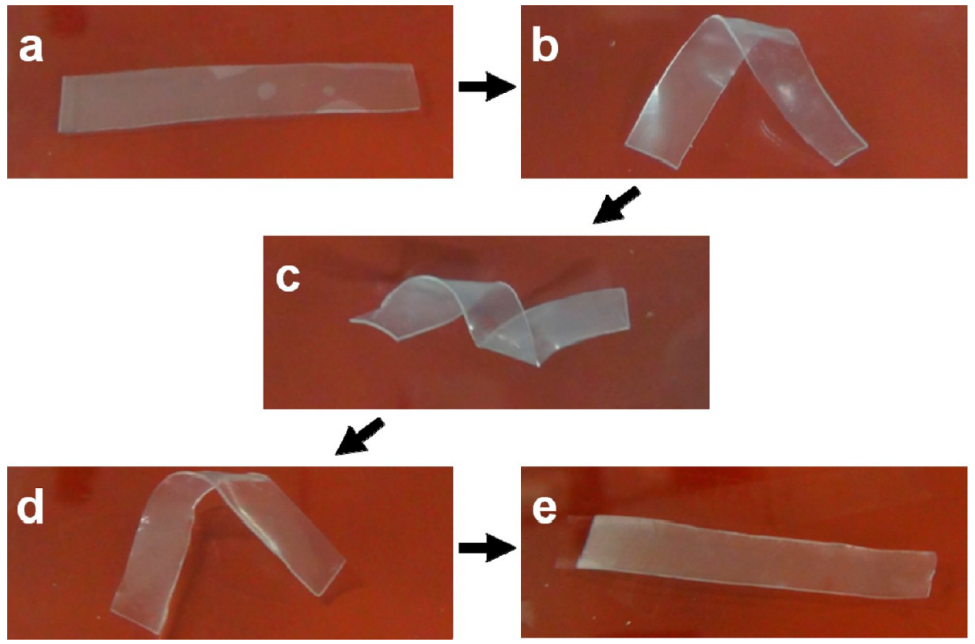

Figure 5. Photographs of cross-linked PE/PP blends with v^{PE} of 50 vol % (ca. 30 × ca. 5 mm^2 at 25.0 °C) initiated by DHBP in the triple SME cycle of deformation (b and c) and recovery (d and e): permanent shape at 25.0 °C (a), first temporary shape at 130.0 °C (b), second temporary shape at 175.0 °C (c), first temporary shape at 130.0 °C (d), and permanent shape at 175.0 °C (e).

cross-linking and DCP−DVB the worst, and DHBP/DCP−DVB was in between. The cross-linking caused lower T_m and smaller ΔH_m. The prepared triple SMPs by cocontinuous immiscible PE/PP blends with v^{PE} of 50 vol % showed pronounced triple SMEs in the DMTA and optical observation. This new strategy of chemically cross-linked immiscible blends with cocontinuous architecture could be used to design and prepare new SMPs with triple SMEs.

AUTHOR INFORMATION

Corresponding Author

*E-mails: dangzm@ustb.edu.cn (Z.-M.D.); lan.ma@ttu.edu (L.M.); guo-hua.hu@univ-lorraine.fr (G.-H.H.).

Notes

The authors declare no competing financial interest.

ACKNOWLEDGMENTS

This work was financially supported by Beijing Municipal Excellent Scholars (2011D009006000005), Open Project of Beijing National Laboratory for Molecular Sciences, NSF of China (Grant Nos. 50977001 and 51073015), The Ministry of Sciences and Technology of China through China-Europe International Incorporation Project (Grant No. 2010DFA51490), State Key Laboratory of Power System (SKLD11KZ04), and the Fundamental Research Funds for the Central Universities (Nos. 06103011 and 06103012). The authors also acknowledge Prof. Dr. Ronald C. Hedden of Texas Tech University, USA for his assistance in the manuscript revision.

REFERENCES

(1) Voit, W.; Ware, T.; Dasari, R. R.; Smith, P.; Danz, L.; Simon, D.; Barlow, S.; Marder, S. R.; Gall, K. *Adv. Funct. Mater.* **2010**, *20*, 162−171.
(2) Yoshida, M.; Lahann, J. *ACS Nano* **2008**, *2*, 1101−1107.
(3) Liu, F.; Urban, M. W. *Prog. Polym. Sci.* **2010**, *35*, 3−23.
(4) Lendlein, A. *J. Mater. Chem.* **2010**, *20*, 3332−3334.
(5) Lendlein, A.; Shastri, V. P. *Adv. Mater.* **2010**, *22*, 3344−3347.
(6) Behl, M.; Razzaq, M. Y.; Lendlein, A. *Adv. Mater.* **2010**, *22*, 3388−3410.
(7) Xie, T. *Polymer* **2011**, *52*, 4985−5000.
(8) Hu, J.; Zhu, Y.; Huang, H.; Lu, J. *Prog. Polym. Sci.* **2012**, *37*, 1720−1763.
(9) Iijima, M.; Kobayakawa, M.; Yamazaki, M.; Ohta, Y.; Kamiya, H. *J. Am. Chem. Soc.* **2009**, *131*, 16342−16343.
(10) Luo, X.; Mather, P. T. *Adv. Funct. Mater.* **2010**, *20*, 2649−2656.
(11) Xu, B.; Fu, Y. Q.; Ahmad, M.; Luo, J. K.; Huang, W. M.; Kraft, A.; Reuben, R.; Pei, Y. T.; Chen, Z. G.; De Hosson, J. Th. M. *J. Mater. Chem.* **2010**, *20*, 3442−3448.
(12) He, Z.; Satarkar, N.; Xie, T.; Cheng, Y.-T.; Hilt, J. Z. *Adv. Mater.* **2011**, *23*, 3192−3196.
(13) Le, H. H.; Schoss, M.; Ilisch, S.; Gohs, U.; Heinrich, G.; Pham, T.; Radusch, H.-J. *Polymer* **2011**, *52*, 5858−5866.
(14) Bae, C. Y.; Park, J. H.; Kim, E. Y.; Kang, Y. S.; Kim, B. K. *J. Mater. Chem.* **2011**, *21*, 11288−11295.
(15) Kumpfer, J. R.; Rowan, S. J. *J. Am. Chem. Soc.* **2011**, *133*, 12866−12874.
(16) Wang, X.; Zhao, J.; Chen, M.; Ma, L.; Zhao, X.; Dang, Z.-M.; Wang, Z. *J. Phys. Chem. B* **2013**, *117*, 1467−1474.
(17) Neffe, A. T.; Hanh, B. D.; Steuer, S.; Lendlein, A. *Adv. Mater.* **2009**, *21*, 3394−3398.
(18) Serrano, M. C.; Carbajal, L.; Ameer, G. A. *Adv. Mater.* **2011**, *23*, 2211−2215.
(19) Chung, T.; Romo-Uribe, A.; Mather, P. T. *Macromolecules* **2008**, *41*, 184−192.
(20) Qin, H.; Mather, P. T. *Macromolecules* **2009**, *42*, 273−280.
(21) Zotzmann, J.; Behl, M.; Hofmann, D.; Lendlein, A. *Adv. Mater.* **2010**, *22*, 3424−3429.
(22) Li, J.; Rodgers, W. R.; Xie, T. *Polymer* **2011**, *52*, 5320−5325.
(23) Raquez, J.-M.; Vanderstappen, S.; Meyer, F.; Verge, P.; Alexandre, M.; Thomassin, J.-M.; Jerome, C.; Dubois, P. *Chem.−Eur. J.* **2011**, *17*, 10135−10143.
(24) Pandini, S.; Passera, S.; Messori, M.; Paderni, K.; Toselli, M.; Gianoncelli, A.; Bontempi, E.; Ricco, T. *Polymer* **2012**, *53*, 1915−1924.
(25) Ma, L.; Zhao, J.; Wang, X.; Chen, M.; Zhao, X.; Wang, Z.; Hedden, R. C. in preparation.

(26) Behl, M.; Bellin, I.; Kelch, S.; Wagermaier, W.; Lendlein, A. *Adv. Funct. Mater.* **2009**, *19*, 102−108.
(27) Behl, M.; Lendlein, A. *J. Mater. Chem.* **2010**, *20*, 3335−3345.
(28) Zotzmann, J.; Behl, M.; Feng, Y.; Lendlein, A. *Adv. Funct. Mater.* **2010**, *20*, 3583−3594.
(29) Ware, T.; Hearon, K.; Lonnecker, A.; Wooley, K. L.; Maitland, D. J.; Voit, W. *Macromolecules* **2012**, *45*, 1062−1069.
(30) Bothe, M.; Mya, K. Y.; Lin, E. J. M.; Yeo, C. C.; Lu, X.; He, C.; Pretsch, T. *Soft Matter* **2012**, *8*, 965−972.
(31) Xie, T.; Xiao, X.; Cheng, Y.-T. *Macromol. Rapid Commun.* **2009**, *30*, 1823−1827.
(32) Ahn, S.-K.; Kasi, R. M. *Adv. Funct. Mater.* **2011**, *21*, 4543−4549.
(33) Xie, T. *Nature* **2010**, *464*, 267−270.
(34) Li, J.; Xie, T. *Macromolecules* **2011**, *44*, 175−180.
(35) Li, J.; Liu, T.; Xia, S.; Pan, Y.; Zheng, Z.; Ding, X.; Peng, Y. *J. Mater. Chem.* **2011**, *21*, 12213−12217.
(36) Li, Y.; Shimizu, H. *Macromolecules* **2008**, *41*, 5339−5344.
(37) Wang, L.; Lau, J.; Thomas, E. L.; Boyce, M. C. *Adv. Mater.* **2011**, *23*, 1524−1529.
(38) Li, L.; Miesch, C.; Sudeep, P. K.; Balazs, A. C.; Emrick, T.; Russell, T. P.; Hayward, R. C. *Nano Lett.* **2011**, *11*, 1997−2003.
(39) Pu, G.; Luo, Y.; Wang, A.; Li, B. *Macromolecules* **2011**, *44*, 2934−2943.
(40) Zhao, J.; Swinnen, A.; Van Assche, G.; Manca, J.; Vanderzande, D.; Van Mele, B. *J. Phys. Chem. B* **2009**, *113*, 1587−1591.
(41) Zhao, J.; Bertho, S.; Vandenbergh, J.; Van Assche, G.; Manca, J.; Vanderzande, D.; Yin, X.; Shi, J.; Cleij, T.; Lutsen, L.; Van Mele, B. *Phys. Chem. Chem. Phys.* **2011**, *13*, 12285−12292.
(42) Salehi, P.; Sarazin, P.; Favis, B. D. *Biomacromolecules* **2008**, *9*, 1131−1138.
(43) Xiang, Z.; Sarazin, P.; Favis, B. D. *Biomacromolecules* **2009**, *10*, 2053−2066.
(44) Li, L.; Shen, X.; Hong, S. W.; Hayward, R. C.; Russell, T. P. *Angew. Chem., Int. Ed.* **2012**, *51*, 4089−4094.
(45) Kolesov, I. S.; Kratz, K.; Lendlein, A.; Radusch, H.-J. *Polymer* **2009**, *50*, 5490−5498.
(46) Brandrup, J.; Immergut, E. H.; Grulke, E. A. *Polymer Handbook*, 4th ed.; Wiley: New York, 1999.
(47) Zhang, H.; Wang, H.; Zhong, W.; Du, Q. *Polymer* **2009**, *50*, 1596−1601.
(48) Cuevas, J. M.; Rubio, R.; German, L.; Laza, J. M.; Vilas, J. L.; Rodriguez, M.; Leon, L. M. *Soft Matter* **2012**, *8*, 4928−4935.